Orbital: The Electronic Journal of Chemistry
journal homepage: www.orbital.ufms.br
e-ISSN 1984-6428

| Vol 12 | | No. 4 | | October-December 2020 |

FULL PAPER

Effect of Nonionic Surfactants on the Crystallinity and Thermal Stability of Poly(vinyl alcohol) Film

Diana M. da Costa[a], Vanessa R. R. Cunha[b], Gustavo F. Perotti[c], Ruan R. Henriques[a], Jorge Amim Jr.[a], and Ana L. Shiguihara[a*]

[a]Universidade Federal do Rio de Janeiro-Campus Macaé, Macaé-RJ, Brasil.
[b]Instituto Federal de Educação, Ciência e Tecnologia de Mato Grosso - Campus Juína, Juína-MT, Brasil.
[c]Universidade Federal do Amazonas-Campus Itacoatiara-ICET, Itacoatiara-AM, Brasil.

Article history: Received: 25 June 2020; revised: 29 August 2020; accepted: 19 November 2020. Available online: 27 December 2020. DOI: http://dx.doi.org/10.17807/orbital.v12i4.1514

Abstract:

In this study, poly(vinyl alcohol) (PVA)/surfactant films were prepared by casting technique. Two nonionic surfactants with different alkyl chain lenghts (Tween 20 and Tween 40) were used. PVA/Tween 20 and PVA/Tween 40 films were characterized by means of Fourier Transform infrared spectroscopy (FTIR), X-ray diffraction (XRD) and thermogravimetric analysis (TGA). FTIR spectra of PVA/Tween films indicated the presence of hydrogen bond interactions between the Tween surfactants and PVA. XRD results showed that the incorporation of Tween 20 and 40 into the PVA film decreased the crystallinity of PVA.TGA curves revealed an increase in the thermal stability of PVA film in the presence of the surfactants.

Keywords: crystallinity; PVA; Tweens

1. Introduction

Poly(vinyl alcohol) (PVA) is a water-soluble polymer that owing to its good mechanical strength, biodegradability, biocompatibility, and resistance to organic solvents has been used in hydrogels, films, adhesives, biomedical and pharmaceutical applications [1]. The aforementioned properties of this polymer are dependent on the crystallinity, molecular weight, method of preparation, degree of polymerization, tacticity, and degree of hydrolysis [1]. In addition, the melting point at 180-230°C and the glass transition temperature (T_g) at 75-85°C of PVA are related to the hydrogen bonding existing between its adjacent chains [1]. The Figure 1 shows polymer structure. In order to improve mechanical, thermal, crystalline properties of PVA, many authors have been investigating the effect of additives such as ionic liquids, ZnO nanoparticles, manganese (II) chloride and glycerin, inorganic salts, carbohydrates, and palm leaf powder [2-7]. Recently, Sun et al. investigated the effect of Tween 20 on the properties of $Ca(NO_3)_2$ doped starch/PVA films and found that Tween 20 increased the water resisting and flexibility of the films [8]. However, to the best of our knowledge, there are no studies in the literature that have described the influence of nonionic surfactants on the thermal and the crystalline properties of pristine PVA film.

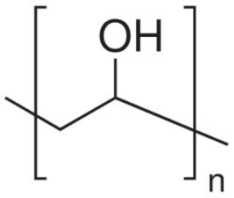

Figure 1. Schematic representation of the PVA chemical structure [1].

Polyoxyethylenesorbitan monolaurate (Tween 20) and polyoxyethylenesorbitan monopalmitate

*Corresponding author. E-mail: anashiguihara@macae.ufrj.br

(Tween 40) are nonionic surfactants composed of fatty acid esters of polyoxyethylene sorbitan [9]. The chemical structures of Tween 20 and 40 consist of two parts: (i) a common polar head referring to a sorbitan ring with ethylene oxide groups attached at three different hydroxyl positions and (ii) a hydrophobic alkyl tail with 10 and 14 -CH_2- groups, respectively [9,10]. Figure 2 exhibits the chemical structures of the surfactants. Owing to the different tail lengths, Tween 20 and 40 present distinct physical properties such as critical micelle concentration (CMC) and hydrophilic-lipophilic balance (HLB). CMC values of Tween 20 and Tween 40 are 0.050 and 0.023 mmol L^{-1} respectively. HLB values of Tween 20 and Tween 40 are 16.7 and 15.6, respectively [10]. Thus, these values of CMC and HLB show that Tween 20 is more hydrophilic than Tween 40. There are many studies in the literature about the application of these surfactants. For example, Tween surfactants can be used in drug delivery formulations [11]. Tween 20 has been applied in the stabilization of oil-water nanoemulsions [12]. Shih et al. prepared gold nanoparticle with Tween 20 and investigated its ability to remove mercury species from a complex matrix [13]. Biswal and Singh investigated the effect of Tween 20 on the interface tension of different oil-water systems in the presence of three different nanoparticles (SiO_2, TiO_2, and ZnO) [14]. In a previous work, a Tween series (Tween 20, 40 and 60) acted as plasticizers for cellulose acetate butyrate (CAB), carboxymethylcellulose acetate butyrate (CMCAB) or cellulose acetate phthalate (CAPh) films, leading to dramatic reduction of glass transition temperature of these polymers [15].

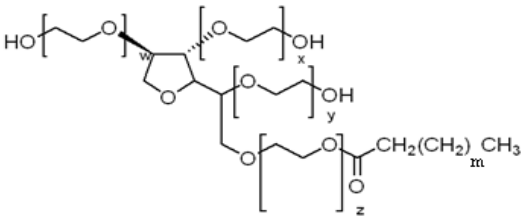

Figure 2. Schematic representation of chemical structures of the surfactants: Tween 20 and Tween 40. These surfactants possess 10 and 14 carbons in alkyl chain, respectively. Where: x + y + z + w = 20 [9,10].

The aim of this work was to develop PVA films in the presence of two different sorbitan-based surfactants (Tween 20 and Tween 40) for potential food packaging applications. Particularly, the effect of the surfactants on the thermal and crystalline properties of PVA film was investigated. The obtained films were characterized using Fourier Transform infrared spectroscopy (FTIR), X-ray diffraction (XRD), and thermogravimetric analysis (TGA).

2. Results and Discussion

Figure 3 reports FTIR spectra for pristine PVA, Tween 20, Tween 40, and PVA/Tween films. FTIR spectra of Tween 20 (Figure 3a) and Tween 40 (Figure 3b) exhibited the typical bands at 3435, 2924, 2859, 1732, and 1104 cm^{-1}. The band at 3435 cm^{-1} was assigned to the OH stretching. Moreover, the bands at 2924, 2859, 1732, and 1104 cm^{-1} were assigned as -CH_3 stretching, -CH_2 stretching, C=O, and C-O-C stretching, respectively [16]. FTIR spectrum of PVA (Figure 3a and b) showed the characteristic absorption bands [17]. The band appearing at 3455 cm^{-1} can be attributed to the stretching of the hydroxyl group (OH) while at 2917 cm^{-1} refers to the C-H stretching from the alkyl group. The bands at 1730 and 1092 cm^{-1} are related to the C=O stretching of the remaining acetate groups and the C-O stretching of PVA, respectively.

The FTIR spectra of the PVA/Tween films (Figure 3a and b) display characteristic bands of PVA, Tween 20, and Tween 40. More specifically, FTIR spectra of PVA/Tween films showed that upon addition of Tween 20 or Tween 40 in PVA, there were significant changes in the OH stretching region. As can be seen in Figure 3a and b, OH band shifted towards lower wavenumber when compared with pristine PVA film. For PVA/Tween 20 film, this band is shifted to 3442 cm^{-1} in X_{T20} = 0.1; 3436 cm^{-1} in X_{T20} = 0.2, and 3435 cm^{-1} in X_{T20} =0.3. In the case of PVA/Tween 40 films, OH band appeared at 3444 cm^{-1} in X_{T40} = 0.1; 3431 cm^{-1} in X_{T40} = 0.2, and 3436 cm^{-1} in X_{T40} = 0.3. These results show the existence of hydrogen bond interactions between the Tween surfactants and PVA. It is suggested that the branched structure of Tween polar head rich in OH and C-O-C groups contributed to interact favorably with the hydroxyl groups from PVA. Vicentini et al. also observed this interaction between Tween 80 and chitosan/PVA/ZnO film

[18]. Furthermore, the overlapped band localized between 1090-1104 cm^{-1} was attributed to both C-O and C-O-C groups of PVA and Tween surfactants in the films, respectively. Considering the FTIR spectra of PVA/Tween 20 and PVA/Tween 40 films with weight fraction of Tween > 0.1, it is possible to observe that the intensity of the characteristic stretching vibration of alkyl groups (-CH_3, -CH_2, and –CH) increased in comparison to the FTIR spectrum of pristine PVA film. This behavior is associated to the increasing amount of Tween surfactant in PVA film.

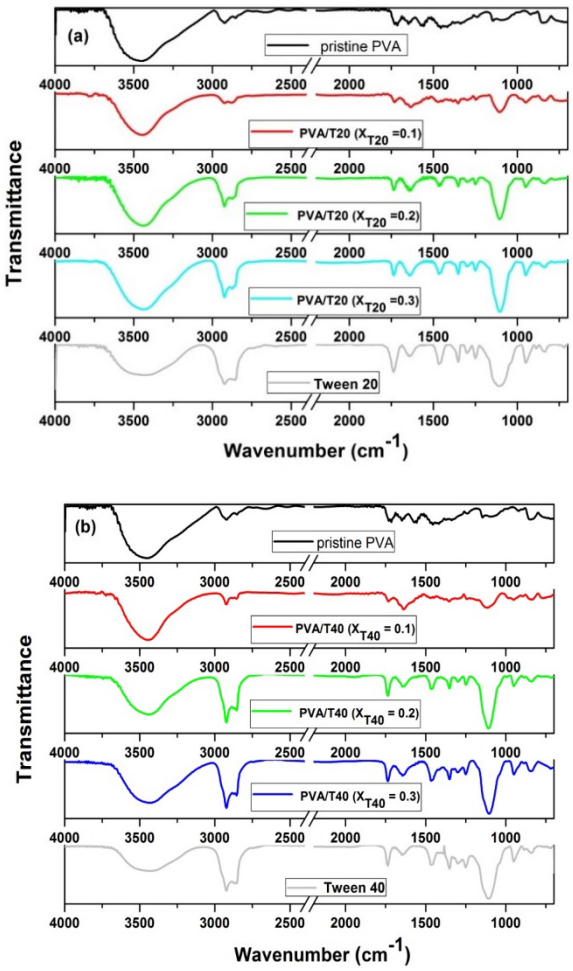

Figure 3. (a) FTIR spectra of PVA, Tween 20, and PVA/Tween 20 films. (b) FTIR spectra of PVA, Tween 40 and PVA/Tween 40 films.

X-ray diffraction (XRD)

XRD patterns of pristine PVA and PVA film as function of the surfactant content (Tween 20 or 40) are depicted in Figure 4. The XRD pattern obtained for pristine PVA exhibited an intense diffraction peak at (2θ) 20° which is a typical peak of the crystalline PVA film [19]. Figure 4a and 4b show the XRD patterns of PVA/Tween 20 and PVA/Tween 40 films having different weight fraction of Tween 20 (W_{T20}) and Tween 40 (W_{T40}). Also, it can be seen that either PVA/Tween 20 or PVA/Tween 40 display similar diffraction peaks of pristine PVA film. However, the inclusion of these nonionic surfactants into the PVA film reduced the intensity of these peaks. These results show that the crystallinity of those PVA/Tween films are intrinsic related to the amount of the Tween surfactants applied when compared to the pristine PVA film. Probably, there is a strong interaction between PVA and the nonionic surfactants that promotes the decrease of crystalline regions in PVA film. PEN et al. also observed that the addition of Tween 20 into chitosan/tea polyphenols films modified the crystal properties of the films [20].

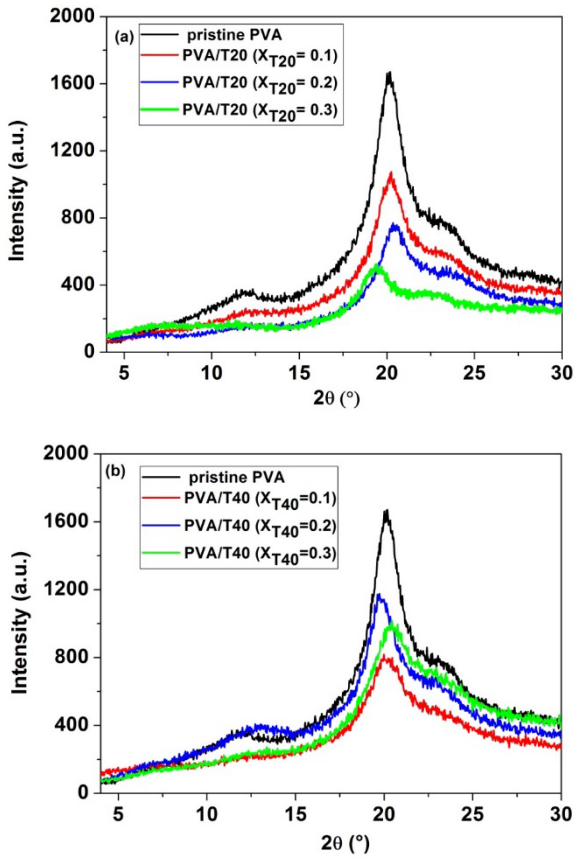

Figure 4. XRD patterns of PVA and PVA/Tween films as a function of surfactant: (a) Tween 20 and (b) Tween 40.

Furthermore, Figure 4a and b show that the crystallinity of PVA/Tween film depends on the W_{T20} and W_{T40}. The relative order of crystallinity of

PVA/Tween 20 film as a function of W_{T20} is: 0.3 < 0.2 < 0.1, this behavior can be attributed to the increase in the interactions between the PVA and Tween 20, thus disrupting more extensively the crystalline regions in PVA/Tween 20 film. In the case of PVA/Tween 40 film, the PVA film which contains W_{T40} = 0.1 had the lower crystallinity between all the PVA/Tween 40 films prepared in this work. Moreover, for W_{T40} > 0.1, PVA/Tween 40 films tended to be more structurally organized in comparison with PVA/Tween 20 films. Therefore, these results show that Tweens with distinct alkyl chain length or HLB values can be used to control the crystallinity of PVA films.

From the experimental data reported in Figure 4, the average crystallite size (D) of PVA with and without the Tween surfactants was determined using the Scherrer equation [21]:

$$D = \frac{K\lambda}{\beta cos\theta}$$

where *K* is a numerical factor, β is the full width at half maximum, θ is the Bragg's angle, and λ is the wavelength of the X-ray radiation. The D values as function of weight fraction of Tween 20 or 40 (X_{Tween}) in PVA/Tween surfactant films are presented in Figure 5. As can be observed in Figure 5, D values of PVA decreased with the increase of X_{Tween}, corroborating the results obtained in Figure 4. In addition, Figure 5 also shows that D values for PVA/Tween 20 film with weight fraction of 0.1 and 0.2 are smaller than PVA/Tween 40 films. However, for X_{Tween} > 0.2, D value is higher for PVA/Tween 20 than PVA/Tween 40. Therefore, these results show that the surfactant alkyl chain length and surfactant content influence the crystal size of PVA film.

Thermogravimetric Analysis (TGA)

The influence of the surfactant content (Tween 20 or 40) on the thermal stability of PVA film was investigated by TGA. The onset thermal decomposition temperature (T_{onset}) and temperature of maximum of mass loss (T_{max}) have been determined from TGA and DTG curves.

Figure 5 shows TGA and DTG curves for Tween 20 and Tween 40. Figure 5a displays that the major weight loss step occurred between 170-440°C and is related to thermal degradation of the surfactants [22, 23]. The T_{onset} values for Tween 20 and 40 were found at about 224 and 216°C, respectively. In addition, DTG curves showed that the thermal degradation of Tween 20 and Tween 40 occurred in two and three steps, respectively. T_{max} values found for Tween 20 are 358 and 526°C and for Tween 40 are 266, 375 and 509°C.

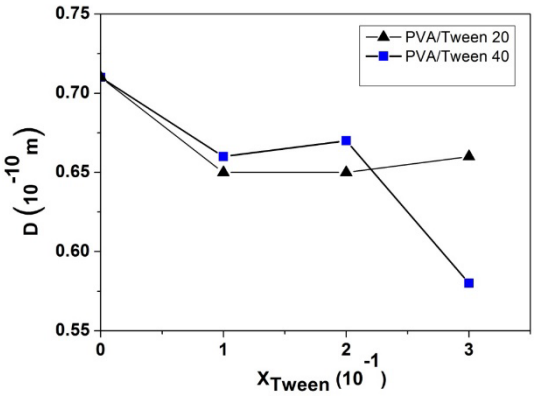

Figure 5. Average crystallite size (D) of PVA as function of weight fraction of Tween 20 or 40 (X_{Tween}) in PVA/Tween surfactant films.

Figures 7 and 8 present TGA and DTG curves of pristine PVA film. TGA curve showed that major weight loss step occurred in the temperature range of 200-370°C and possesses T_{onset} value at 251°C. PVA thermal degradation occurred in four steps as it can be seen by DTG curve (Figure 7). The first step has T_{max} = 100°C and corresponds to the release of water molecules. The following three degradation steps have T_{max} values at 291, 434, and 500°C and can be attributed to the thermal degradation of PVA chains [24].

In the case of PVA/Tween 20 and PVA/Tween 40 films, TGA and DTG curves presented thermogravimetric behavior different of those obtained for pristine PVA film, as shown in Figure 7 and 8. The T_{onset} value corresponding to the second degradation step of PVA/Tween 20 films containing 0.1, 0.2 and 0.3 (as weight fraction X) of Tween 20 were found at 243, 252, and 252°C, respectively. For PVA/Tween 40 films with 0.1, 0.2 and 0.3 (as weight fraction X) of Tween 40, the obtained T_{onset} values were: 256, 250 and 254°C, respectively. Compared to the T_{onset} of pristine PVA (T_{onset} = 251°C), these results show that Tween 40 promotes a higher thermal stability for PVA film than Tween 20, except for weight fraction of Tween 40 of 0.2. Probably, the

hydrogen bond interactions between the PVA-Tween 40 and the higher alkyl chain length of the Tween 40 in comparison with Tween 20 contributed to this behavior.

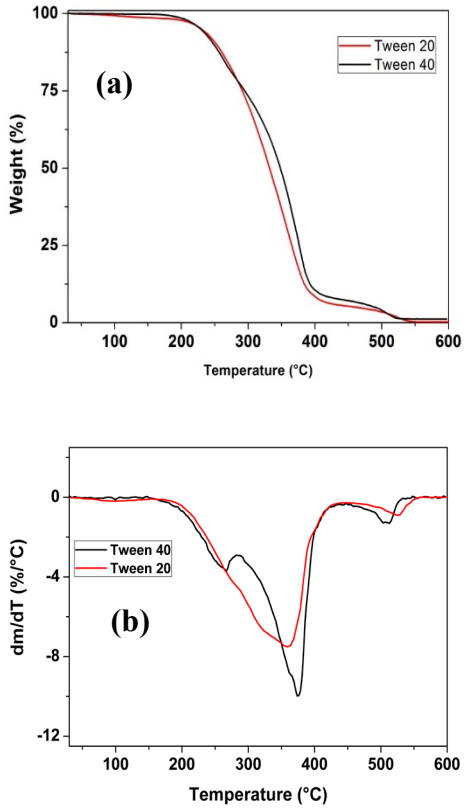

Figure 6. (a) TGA and (b) DTG curves for Tween 20 and 40.

Table 1 shows T_{max} values obtained from DTG curves for each degradation step of PVA, PVA/Tween 20 and PVA/Tween 40 films. The first degradation step can be associated to the removal of water molecules from all samples. The following degradation steps are related to the decomposition of PVA and surfactants in the film. Moreover, it is important to observe in Table 1 that T_{max} values of PVA/Tween 20 and PVA/Tween 40 films for the second degradation step shifted significantly toward higher temperatures than those of pristine PVA film, except for PVA/Tween 20 film with 0.1 of Tween 20. Therefore, the addition of Tween surfactants into PVA film improved the thermal stability of PVA film. This behavior is probably due to the hydrogen bond interactions between PVA and surfactants.

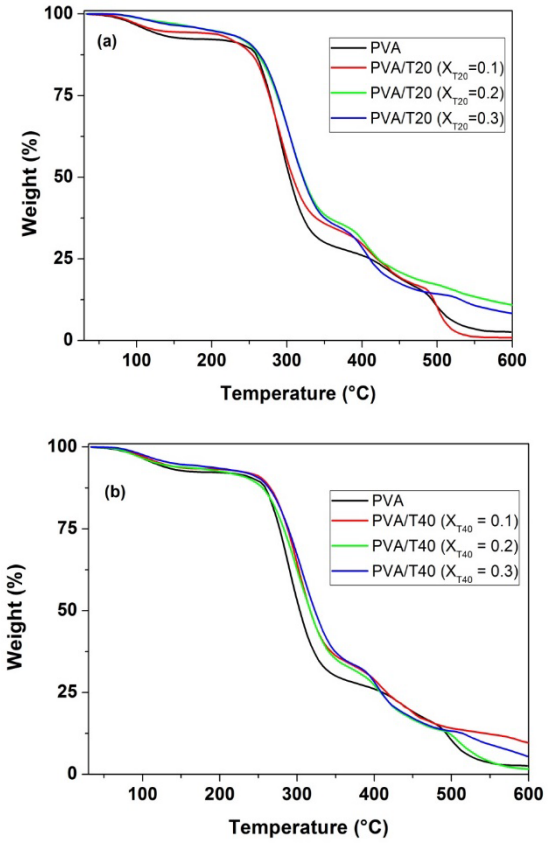

Figure 7. TGA curves for PVA and PVA/Tween films a function of surfactant: (a) Tween 20 and (b) Tween 40.

Table 1. T_{max} values for pristine PVA, PVA/tween 20 and PVA/tween 40 films as a function of degradation step.

Sample	T_{max} (°C) for each degradation step			
Pristine PVA	100 (1)	291 (2)	434 (3)	500(4)
PVA/Tween 20 (0.1)	96 (1)	288 (2)	422 (3)	502(4)
PVA/Tween 20 (0.2)	99 (1)	302 (2)	408 (3)	-
PVA/Tween 20 (0.3)	109 (1)	303 (2)	404 (3)	538 (4)
PVA/Tween 40 (0.1)	99 (1)	300 (2)	421 (3)	-
PVA/Tween 40 (0.2)	99 (1)	302 (2)	407 (3)	515(4)
PVA/Tween 40 (0.3)	99 (1)	306 (2)	405 (3)	530(4)

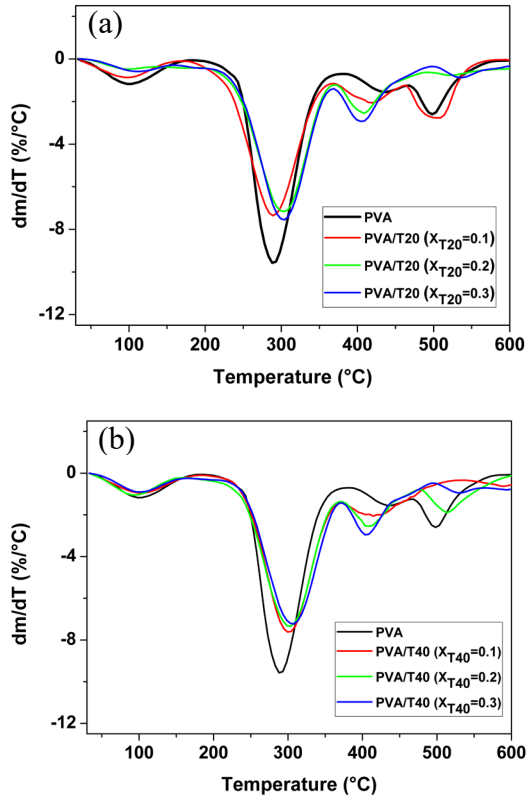

Figure 8. DTG curves for PVA and PVA/Tween films a function of surfactant: (a) Tween 20 and (b) Tween 40.

3. Material and Methods

3.1 Materials

For this present study, poly(vinyl alcohol) (PVA) (average M_w 31-50 Kg mol^{-1}, 98-99% hydrolyzed) and the surfactants: polyoxyethylenesorbitan monolaurate (Tween 20) and polyoxyethylenesorbitan monopalmitate (Tween 40) were purchased from Sigma-Aldrich. Polymer and surfactants were used as received.

3.2 Sample preparation

Mixtures of PVA with Tween 20 and 40 were prepared using casting technique from aqueous solutions at 60ºC. The samples were dried until constant mass. The content of surfactants (as weight fraction X) in the dried mixture with PVA ranged from 0.1 to 0.3.

3.3 Characterization

3.3.1 Fourier Transform Infrared Spectroscopy (FTIR)

FTIR spectra of the samples were obtained using a Shimadzu IRAffinity-1spectrometer using KBr pressing method. The analysis was carried out in the spectral range of 400–4000 cm^{-1} with 4 cm^{-1} resolution and 32 scans.

3.3.2 X-ray diffraction (XRD)

XRD patterns of the samples were recorded in a Rigaku MiniFlex diffractometer (Japan), using Cu kα radiation at 30 kV and 15 mA, over an angular range of 4-16° with a step size of 0.02°.s^{-1}.

3.3.3 Thermogravimetry analysis (TGA)

TGA measurements were carried out using a Netzsch equipment model TGA/DSC 490 PC Luxx. The samples were heated from 30 to 600°C at a heating rate of 10 ºC. min^{-1} under synthetic air flow of 50 mL min^{-1}.

4. Conclusions

In this work, films of PVA with two nonionic surfactants (Tween 20 and 40) were obtained by solvent casting method and characterized by XRD, TGA, and FTIR. XRD measurements revealed that the surfactants reduce the crystallinity of PVA film. TGA curves showed that PVA/Tween 20 and PVA/Tween 40 films are thermally more stable when compared to pristine PVA. FTIR spectra of PVA/surfactants showed that the hydrogen bonding interactions between the PVA and the surfactants are the driving force for the increase of the thermal stability and the reducting of the crystallinity of PVA film. Therefore, the obtained results showed that the Tween 20 and 40 are promising additives to PVA film.

Acknowledgments

The authors acknowledge FAPERJ for financial support.

References and Notes

[1] Aslam, M.; Kalyar, M. A.; Raza, Z. A. *Polym. Eng. Sci.* **2018**, *58*, 2119. [Crossref]

[2] Zhang, P.; Peng, L.; Li, W. *e-Polymers* **2008**, *8*, 1. [Crossref]

[3] Abd-Elrahman, M. I. *Nanoscale Microscale Thermophys. Eng.* **2013**, *7*, 194. [Crossref]

[4] Jia, P.; Zhang, M.; Bo, C.; Hu, L.; Zhou, Y. *Pol. J. Chem. Technol.* **2015**, *17*, 29. [Crossref]

[5] Tretinnikov, O. N.; Zagorskaya, S. A. *J. Appl. Spectrosc.* **2012**, *78*, 904. [Crossref]

[6] Dai, H.; Wang, J.; Liu, N. *J. Vinyl Addit. Technol.* **2019**, *25*, 181. [Crossref]

[7] Patel, A. K.; Bajpai, R.; Keller, J. M. *Microsyst. Technol.* **2014,** *20*, 41. [Crossref]

[8] Sun, Y.; Lin, Z.; Jiang, X.; Hou, L. *Starch* **2018**, *70*, 1. [Crossref]

[9] Kerwin, B. A. *J. Pharm. Sci.* **2008**, *97*, 2924. [Crossref]

[10] Hait, S. K.; Moulik, S. P. *J. Surfactants Deterg.* **2001**, *4*, 303. [Crossref]

[11] Kaur, G.; Mehta, S. K. *Int. J. Pharm.* **2017**, *529*,134. [Crossref]

[12] Cheong, A. M.; Nyam, K. L. *J. Food Eng.* **2016**, *183*, 24. [Crossref]

[13] Shih, Y-C.; Ke, C-Y.; Yu, C-J.; Lu, C-Y; Tseng, W-L. *ACS Appl. Mater. Interfaces* **2014**, *6,* 17437. [Crossref]

[14] Biswal, N. R.; Singh, J. K. *RSC Adv.* **2016**, *6*, 113307. [Crossref]

[15] Amim, J.; Blachechen, L.S.; Petri, D. F. S. *J. Therm. Anal. Calorim.* **2012**, *107*, 1259. [Crossref]

[16] Ortiz-Tafoya, M. C.; Tecante, A. *Data in Brief* **2018**, *19*, 642. [Crossref]

[17] Santos, C.; Silva, C. J.; Buttel, Z.; Guimarães, R.; Pereira, S. B.; Tamgnini, P.; Zille, A. *Carbohydr. Polym.* **2014**, *99*, 584. [Crossref]

[18] Vicentini, D. S.; Smania Jr., A.; Laranjeira, M. C. M. *Mater. Sci. Eng.* C **2010**, *30*, 503. [Crossref]

[19] Mohamed, S. A,; Al-Ghamdi, A. A.; Sharma, G. D.; El Mansy, M. K. *J. Adv. Res.* **2014**, *5*, 79. [Crossref]

[20] Peng, Y.; Wang, Q.; Shi, J.; Chen, Y.; Zhang, X. *Food Sci. Technol.* **2020**, *40*, 162. [Crossref]

[21] Holzwarth, U.; Gibson, N. *Nat. Nanotechnol.* **2011**, *6*, 534. [Crossref]

[22] Kishore, R. S. K.; Pappenberger, A.; Dauphin, I. B.; Ross, A.; Buergi, B.; Staempfli, A.; Mahler, H-C. *J. Pharm. Sci.* **2011**, *100*, 721.

[23] de Lima, B. R. M.; do Nascimento, N. M. P.; Zamian, J. R; da Costa, C. E. F.; do Nascimento, L. A. S.; Carneiro-Moreira, S. G.; da Rocha Filho, G. N. *Environ. Chem. Lett.* **2020**, *18*, 1413. [Crossref]

[24] Zhou K.; Jiang, S.; Bao, C.; Song, L.; Wang, B.; Tang, G.; Hu, Y.; Gui, Z. *RSC Advances* **2012**, *2*, 11695. [Crossref]